Reduction in Inspection Costs for Dynamic Sensitive Steel Structures by Modal Based Fatigue Monitoring

Henrik P. Hjelm
Structural Vibration Solutions A/S
Novi Science Park, Niels Jernes Vej 10, DK-9220 Aalborg East, Denmark
h.hjelm@stofanet.dk

John D. Sørensen
Department of Building Technology and Structural Engineering
Aalborg University, Sohngaardsholmsvej 57, DK-9000 Aalborg, Denmark
i6jds@civil.aau.dk

Rune Brincker
Department of Building Technology and Structural Engineering
Aalborg University, Sohngaardsholmsvej 57, DK-9000 Aalborg, Denmark
i6rb@civil.aau.dk

Jesper Graugaard-Jensen
Structural Vibration Solutions A/S
Novi Science Park, Niels Jernes Vej 10, DK-9220 Aalborg East, Denmark
jespergj@stofanet.dk

Kasper Munch
Structural Vibration Solutions A/S
Novi Science Park, Niels Jernes Vej 10, DK-9220 Aalborg East, Denmark
k_munch@stofanet.dk

Abstract

In risk based inspection planning the number of planned inspections directly depends on the uncertainty on the load history. In this paper it is shown how this uncertainty can be reduced by modal based fatigue monitoring. The technique is based on continuously measuring of the accelerations in few points of the structure. The accelerations are integrated to obtain the displacement and a modal decomposition of the obtained displacements is performed. The relation between the modal coordinates and the stress history in an arbitrary point of the structure is established by a calibrated finite element model. The technique has been applied on a wind loaded lattice pylon structure and compared with strain gauges measurements, showing that the uncertainty on the presented technique is quite small. It is shown that if the technique is applied to an offshore steel structure, then the number of required inspections may be reduced with more than 50%.

1. Introduction

The basic idea of inspection planning is to plan inspections and maintenance activities such that legislative requirements to the safety of personnel and environment for the considered structure are fulfilled. At the same time the overall costs of inspections, repairs and failures are minimized.

Reliability and risk based inspection planning (RBI) for offshore facilities have been developed over the last two decades and recently generic and simplified approaches for RBI have been formulated. These approaches facilitate a generic modeling of fatigue sensitive structural details in terms of parameters, which are commonly applied in deterministic design of structures. One of these parameters X_s models the uncertainty related to the load history, the structures transfer function and the Stress Concentration Factors (SCF). In this paper a new technique of determining stress histories is introduced; modal based fatigue monitoring, which by measurements efficient reduces the uncertainty, related to the load history and the transfer

function. By applying this technique on offshore structures and combining it with RBI the value of X_s is reduced and the frequency of the inspections can be reduced.

By determining the stress histories in structures by modal based fatigue monitoring two important advantages are introduced. First, the method is based on measurements with accelerometers, which are known as reliable for long time measurements. Second, by a calibrated finite element model the stress history can be calculated in any arbitrary point of a structure when accelerations are measured in only a few points of the structure.

The theory of modal based fatigue monitoring is explained in details and validated through experiments in Graugaard-Jensen et al. [1]. In this paper the theory is summarized and the main results of one experiment are shown. More results can be found in Graugaard-Jensen et al. [2]. The theory of risk based inspection planning is given according to Faber et al. [3].

2. Theory of Generic Risk Based Inspection Planning

2.1. Fatigue Strength

In general the fatigue strength of structures can be calculated by a SN-curve approach or a fracture mechanics (FM) approach.

2.1.1. SN-Curve Approach

In the SN-curve approach it is assumed that the SN-curve is bilinear:

$$N = K_1 \left(\frac{\Delta s}{\left(T / T_{ref}\right)^{\alpha^*}} \right)^{-m_1} \quad \text{for } N \le N_C \tag{1}$$

$$N = K_2 \left(\frac{\Delta s}{\left(T / T_{ref}\right)^{\alpha^*}} \right)^{-m_2} \quad \text{for } N > N_C \tag{2}$$

where

Δs	Stress range
N	Number of cycles to failure
K_1, m_1	Material parameters for $N \le N_C$
K_2, m_2	Material parameters for $N > N_C$
T	Thickness
T_{ref}	Reference thickness
α^*	Scale exponent

Further, it is assumed that the total number of stress ranges for a given fatigue critical detail can be grouped in n_σ groups / intervals such that the number of stress ranges in group i is n_i per year.

The code-based design equation is written:

$$G = 1 - \sum_{s_i \ge \Delta s_C} \frac{n_i T_F}{K_1^C s_i^{-m_1}} - \sum_{s_i < \Delta s_C} \frac{n_i T_F}{K_2^C s_i^{-m_2}} = 0 \tag{3}$$

where

$s_i = \dfrac{Q_i}{z} \dfrac{1}{\left(T / T_{ref}\right)^{\alpha^*}} = \dfrac{Q_i}{z^*}$ is the stress range in group i

Δs_C	Stress range corresponding to N_C
Q_i	Action effect (proportional to stress range s_i in group i)
z	Design parameter
z^*	Modified design parameter taking into account thickness effects
K_i^C	Characteristic value of K_i (mean of log K_i minus two standard deviations of log K_i)
T_F	Fatigue lifetime, $T_F = T_L \cdot FDF$
T_L	Service lifetime
FDF	Fatigue Design Factor. Typically values of FDF are 1, 3, 5 and 10 depending on the consequence of failure and accessibility of the joint, cf. NORSOK [4].

The design parameter z^* is determined from the design equation (3). Next, the reliability index (or the probability of failure) is calculated using this design value and the limit state function associated with (3). The coefficient of variation COV_{load} models the uncertainty on the load history, transfer function (e.g. foundation stiffness and damping). COV_{SCF} models the uncertainty in the stress concentration factors (SCF) and local joint flexibilities (LFJ), see below.

The limit state equation can be written:

$$g = 1 - \sum_{s_i \ge \Delta s_C} \frac{n_i T_L}{K_1 s_i^{-m_1}} - \sum_{s_i \ge \Delta s_C} \frac{n_i T_L}{K_2 s_i^{-m_2}} \tag{4}$$

where

$s_i = X_S \dfrac{Q_i}{z^*}$ is the stress range in group i

X_S	Stochastic variable modeling model uncertainty related to load history, transfer function and SCF. X_S is Log-Normal distributed with mean value = 1 and $COV = \sqrt{COV_{load}^2 + COV_{SCF}^2}$
K_i	log K_i is modeled by a Normal distributed stochastic variable according to a specific SN-curve. T- and F-curves are used

2.1.2. FM Approach

The crack growth is modeled by a fracture mechanical model assuming that the crack can be modeled by a 2-dimensional semi-elliptical crack. It is assumed that the

fatigue life may be represented by a fatigue initiation life and a fatigue propagation life.

The following model is used:

$$N = N_I + N_P \tag{6}$$

where

N	Number of stress cycles to failure
N_I	Number of stress cycles to crack propagation
N_P	Number of stress cycles from initiation to crack through

The number of stress cycles from initiation to crack through is determined on the basis of a two-dimensional crack growth model. The crack is assumed to be semi-elliptical with length $2c$ and depth a, cf. Figure 1.

The crack growth can be described by the following two coupled differential equations

$$\begin{aligned} \frac{da}{dN} &= C_A\left(\Delta K_A\right)^m \qquad a\left(N_0\right) = a_0 \\ \frac{dc}{dN} &= C_C\left(\Delta K_C\right)^m \qquad c\left(N_1\right) = c_0 \end{aligned} \tag{7}$$

where

C_A, C_C, m	Material parameters
a_0, c_0	Describe the crack depth a and crack length c, respectively, after N_I cycles
ΔK_A, ΔK_C	The stress intensity ranges. ΔK_A and ΔK_C are obtained based on the models in Newmann & Raju [5] and Smith & Hurworth [6].

The sum of the membrane stresses σ_t and the bending stresses σ_b is taken as

$$\sigma_t + \sigma_b = \Delta\sigma \tag{8}$$

It is assumed that the ratio between bending and membrane stresses is η implying that

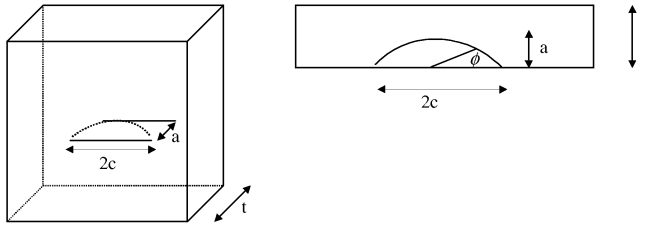

Figure 1 *Semi-elliptical crack in a plate under tension or bending fatigue loads.*

$$\sigma_t = \frac{1}{\eta+1}\Delta\sigma \quad \text{and} \quad \sigma_b = \frac{\eta}{\eta+1}\Delta\sigma \tag{9}$$

Load shedding (linear moment release) is introduced as described in Aaghaakouchak et al. [6].

The stress range $\Delta\sigma$ is obtained from

$$\Delta\sigma = Z_{load} + Z_{SCF}\Delta\sigma^e \tag{10}$$

where

Z_{load} and Z_{SCF}	model uncertainties
$\Delta\sigma^e$	equivalent stress range

$$\Delta\sigma^e = \left[\frac{1}{n}\sum_{i=1}^{n_\sigma} n_i \Delta\sigma_i^m\right]^{1/m} \tag{11}$$

The total number of stress ranges per year n is

$$n = \sum_{i=1}^{n_\sigma} n_i \tag{12}$$

In the assessment of the equivalent constant stress range the effect of a possible lower threshold value ΔK_{TH} on the crack growth inducing stress intensity factor ΔK has not been taken directly into account. This effect is assumed implicitly accounted for by evaluation of Equation (11) using the appropriate SN-curve exponent m.

The crack initiation time N_I is modeled as Weibull distributed with expected value μ_0 and coefficient of variation equal to 0.35, see e.g. Lassen [7].

The limit state function is written

$$g(x) = N - nt \tag{13}$$

where t is time in the interval from 0 to the service life T_L .

In order to model the effect of different weld qualities two different values of the crack depth at initiation a_0 are used; 0.1 mm and 0.5 mm corresponding approximately to high and low material control. The corresponding assumed crack length c_0 is 5 times the crack depth. The critical crack depth a_c is taken as the member thickness.

2.2. Implementation of Generic RBI in iPlan

In inspection planning a model is needed which gives a measure of the crack size, since an inspection results in a measured crack size, if a crack is detected. Therefore the fracture mechanics model is calibrated to the SN-curve model by requiring that the reliability index as function of time for the two models should be as close as possible. The reliability indices can be obtained using either FORM/SORM methods or using Monte Carlo simulation.

The inspection planning is performed on the basis of the assumption that no cracks are detected by the inspections. Further, an inspection is carried out when the reliability with respect to the considered event decreases below a given acceptable limit.

The inspections may be performed by e.g. Magnetic Particle Inspection, Eddy Current or Close Visual Inspection. Each of these inspection methods are associated with a given probability of detection on the size of the crack and depending on whether the inspection is carried out above or below water. As mentioned it is assumed that no crack is detected by the inspection, i.e. the crack is smaller than the detectable crack size. This event can be modeled by the following limit state function

$$h = a(t) - a_d \tag{14}$$

where a_d is the depth of the detectable crack.

The distribution of the size of the detectable crack or the so-called POD-curve (Probability of Detection) depends on the inspection method. The distribution of the detectable crack can be modeled by an upward bounded Exponential distribution

$$F_{a_d}(a_d) = P_0(1 - \exp(-a/\lambda)) \tag{15}$$

where λ and P_0 are model parameters which may be determined by tests.

Following the approach outlined above it is possible to establish so-called generic inspection plans, cf. Faber et al. [3]. The idea is to establish pre-fabricated inspection plans for different joint types designed for different fatigue lives. For a given

- type of fatigue sensitive detail – and thereby code-based SN-curve
- fatigue strength measured by *FDF* (Fatigue Design Factor)
- importance of the considered detail for the ultimate capacity of the structure, measured by e.g. *RSR* (Reserve Strength Ratio)
- inspection, repair and failure costs

the optimal inspection plan i.e. the inspection times, the inspection qualities and the repair criteria, can be determined.

This inspection plan is generic in the sense that it is representative for the given characteristics of the considered detail, i.e. SN-curve, *FDF*, *RSR* and the inspection, repair and failure costs.

For practical application of the methodology, a database iPlan, used by Maersk Oil and Gas, has been developed, cf. Faber et al. [3]. The iPlan database is developed to obtain inspection plans from interpolation between the pre-defined generic plans and facilitates the straightforward production of large numbers of inspection plans for structural details subject to fatigue deterioration.

3. Theory of Modal Based Fatigue Monitoring

So far it is outlined how the number of planned inspections in RBI directly depends on the uncertainty on e.g. the load history included in the parameter X_S. In this section it is explained how this uncertainty can be reduced by modal based fatigue monitoring.

The accelerations of a structure, exposed to a stochastic loading, are measured in a few easily accessible points of the structure. A modal identification is performed to obtain the natural frequencies f_{exp} and mode shapes $\mathbf{\Phi}_{\text{exp}}$ of the structure. The identification may be performed by e.g. Stochastic Subspace Identification (SSI), cf. Van Overschee and De Moor [8], or Frequency Domain Decomposition (FDD), cf. Brincker et al. [9]. The FDD is used in this paper as implemented in the ARTeMIS Extractor software. The FDD is based on calculation of Spectral Density Matrices of the measured data series by discrete Fourier transformation. For each frequency line the Spectral Density Matrix is decomposed into auto spectral functions corresponding to a single degree of freedom system (SDOF).

A finite element model is calibrated to obtain

$$\mathbf{\Phi}_{\text{exp}} = \mathbf{A}\ \mathbf{\Phi}_{\text{FE}} \tag{16}$$

where $\mathbf{A}$ is an observation matrix containing zeros and ones.

The measured accelerations are integrated twice to obtain the displacements $\mathbf{y}_{\text{exp}}(t)$. The integration is performed by use of Simpson's Rule, cf. Kreyszig [9], and the resulting numerical drift is removed by digital high-pass filtering, e.g. by use of Butterworth filters.

The obtained displacements $\mathbf{y}_{\text{exp}}(t)$ are expanded in modal coordinates $\mathbf{q}(t)$ by use of either the experimental mode shapes $\mathbf{\Phi}_{\text{exp}}$

$$\mathbf{y}_{\text{exp}}(t) = \mathbf{\Phi}_{\text{exp}}\ \mathbf{q}(t) \tag{17}$$

or numerical mode shapes $\mathbf{\Phi}_{\text{FE}}$

$$\mathbf{y}_{\text{exp}}(t) = \mathbf{A}\ \mathbf{\Phi}_{\text{FE}}\ \mathbf{q}(t) \tag{18}$$

From the modal coordinates and the numerical mode shapes, the response $\mathbf{y}_{\text{FE}}(t)$ in any arbitrary point of the structure is simply calculated by

$$\mathbf{y}_{\text{FE}}(t) = \mathbf{\Phi}_{\text{FE}}\ \mathbf{q}(t) \tag{19}$$

and the strains and far field stresses can be calculated in any point of the structure by traditional finite element calculations. The hot spot stresses are calculated by

applying the finite element relationship between the far field stresses and the hot spot stresses.

Use of the experimental mode shapes in the modal expansion may seem as the most obvious, since the response is experimental determined, but in some cases equation (16) cannot be fulfilled. If e.g. the structure is symmetric, some of the identified mode shapes may be unstable and the direction may differ from the numerical mode shapes. In such a case, the modal expansion must be performed by use of the numerical mode shapes. However, it is important that the FE-model is always correct calibrated. The calibration is checked by comparison of the experimental and numerical natural frequencies and by calculating the Modal Assurance Criteria (MAC) between the experimental and numerical mode shapes. The MAC varies between zero and one, where one denotes full correlation of the modes. The MAC between the *i*th experimental and numerical mode shape is calculated as

$$\mathrm{MAC}(\Phi_{\mathrm{exp},i},\Phi_{\mathrm{FE},i}) = \frac{\left|\Phi_{\mathrm{exp},i}\Phi_{\mathrm{FE},i}\right|^2}{(\Phi_{\mathrm{exp},i}^{\mathrm{T}}\Phi_{\mathrm{exp},i})(\Phi_{\mathrm{FE},i}^{\mathrm{T}}\Phi_{\mathrm{FE},i})} \qquad (20)$$

The MAC between $\boldsymbol{\Phi}_{\mathrm{exp}}$ and $\boldsymbol{\Phi}_{\mathrm{FE}}$ should generally be high to obtain accurate results, unless $\boldsymbol{\Phi}_{\mathrm{exp}}$ is unstable.

If the number of mode shapes of the system equals the measured degrees of freedom, then equation (17) or (18) is solved directly. If the number of measured degrees of freedom exceeds the number of mode shapes, the equation is over determined and is solved by linear regression, e.g. the Least Square method.

If the number of mode shapes exceeds the number of measured degrees of freedom the equation is under determined and must be divided into sub-systems. The dividing into sub-systems may be performed by digital filtering or directly in frequency domain by considering the same problem frequency range by frequency range. The division into sub-systems shall furthermore ensure that mode shapes with high correlation is not included in the same sub-system. High correlated mode shapes included in the same sub-system may result in error on the calculated modal coordinates, resulting in large errors on the following calculation of the stress history, cf. Graugaard-Jensen et al. [1]. The correlation is checked by calculating the MAC.

4. Implementation of Modal Based Fatigue Monitoring in Generic RBI

Since the modal based fatigue monitoring requires acceleration measurements it cannot be implemented in the generic RBI in the design phase. For this reason the stress history has to be determined in traditional manner (e.g. by simulation) in the design phase and the RBI is used to minimize the overall design and inspection costs.

When the structure is build the accelerometers are mounted and the modal properties of the structures are determined from the initial measurements. Next, a finite element model is calibrated and software is setup, calculating the accumulated damage or equivalent stress ranges in the considered joints from the continuous acceleration measurements. From e.g. one year measurements a new and better estimate of the equivalent stress ranges is obtained, giving a smaller value of COV_{load}. Based on these new values the inspection plans can be updated, resulting in fewer inspections.

5. Experimental Verification of Modal Based Fatigue Monitoring

In Graugaard-Jensen et al. [1] the modal based fatigue monitoring is experimental verified. In this section a short review of the experiment and the results is given.

5.1. Introduction to Experiment

The experiment is conducted to a 20 m high welded lattice pylon structure, located near the Structural Research Laboratory of Aalborg University. The structure has a constant width of 0.9 m and plywood plates are mounted on the upper 1.5 m of the structure to increase the wind load. The purpose of the experiment is to demonstrate that the far field stress history in the structure can be calculated in any point with sufficient accuracy by modal based fatigue monitoring. This is demonstrated by simultaneous measuring strains in two sections on the lower part of the structure and accelerations on the upper part of the structure.

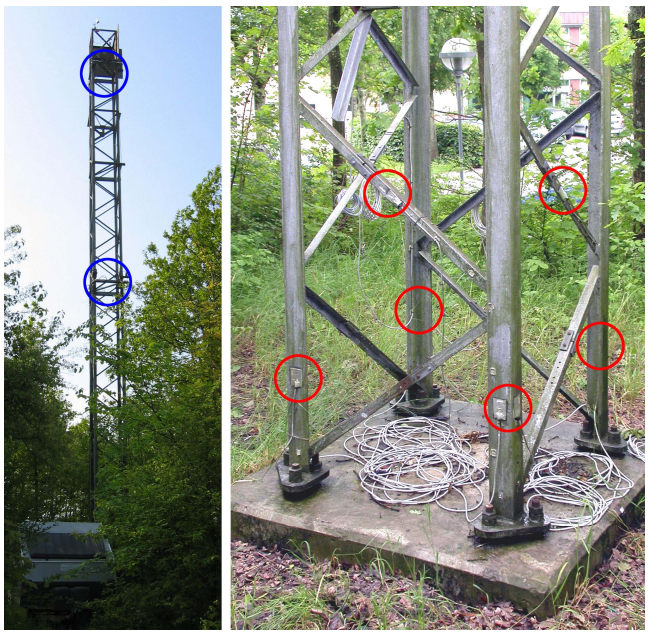

Figure 2 *Lattice pylon structure. (Left) entire structure, (right) base of structure. The blue and red circles indicate the location of accelerometers and strain gauges, respectively.*

The stresses in the lower part of the structure are subsequently calculated from the strain gauge measurements and from the acceleration measurements (modal based fatigue monitoring), and the stress histories are compared.

For simplicity, in the rest of this paper the stress calculations, based on the strain gauges measurements, are referred to as "measured stresses", and the stress calculations, based on the acceleration measurements (modal based fatigue monitoring), are referred to as "calculated stresses".

The vibration monitoring system, composed of 6 Shaevitz accelerometers and 8 single 120 Ω complimentary gauges, was installed on the lattice structuer for one month in the spring 2004. Three accelerometers were mounted at the top of the structure, three accelerometers near the middle of the structure and the 8 strain gauges were mounted 0.5 m above the support of the structure. Two of the strain gauges were mounted on diagonals and the rest of the strain gauges were mounted on the legs of the structure. All strain gauges were measuring in the direction of the profiles.

The monitoring system was initially setup to sample continuously one hour every forth hour, and during periods with high wind speed the monitoring was running continuously in several hours. In all, 223 hours of measurements was recorded. All measurements were sampled with 100 Hz.

The structure is modeled in the finite element program StaadPro using beam elements with six d.o.f. per node. The model is calibrated by applying springs in the support of the model.

5.2. Results of Experiment

Eight modes are identified from 30 minutes measurement series. In Figure 3 the results of the modal identification by FDD is plotted. In Table 2 the experimental and numerical determined natural frequencies are compared and MAC between $\mathbf{\Phi}_{FE}$ and $\mathbf{\Phi}_{exp}$ are calculated. In Figure 6 the mode shapes are plotted.

The modal identification is performed on different 30 minutes measurements series with different wind speeds and wind directions. By comparison the identified mode shapes from the different series, it is found that mode shape 1 and 2 are not stable. For this reason, the MAC between the experimental and numerical mode shape 1 and 2 are low, and the modal expansion must be done using the numerical mode shapes.

The numerical drift resulting from the integration is removed by a 5th order 0.2 Hz low-pass Butterworth filter.

Since the results are used in fatigue analysis it is important to include all the modes that contribute significantly to the fatigue damage. These modes are identified by calculating the damage vs. the number of modes. For instance, the modes of higher order are filtered out one by one (or in pairs) by low-pass filtering and for each filter step the accumulated damage is calculated. If the damage is not reduced significantly by a low-pass filtering the filtered modes can be left out. In this manner it is found that only the two first modes of the lattice structure are participating significantly to the fatigue damage. Therefore, the measurements are run through an 8th order 5 Hz low-pass Butterworth filter and only mode shape 1 and 2 are used in the calculations.

In Figure 4 an example of a 10 min. stress history for channel 1 (leg) is shown, comparing the measured and calculated stresses. The figure shows that the stress histories have been calculated with great accuracy. In Graugaard-Jensen et al. [1] it is found that main part of the deviation between the measurements and calculations is caused by a small error on the estimated static response. This error can be minimized by expanding the static displacements in the complete set of mode shapes, thus including high order mode shapes.

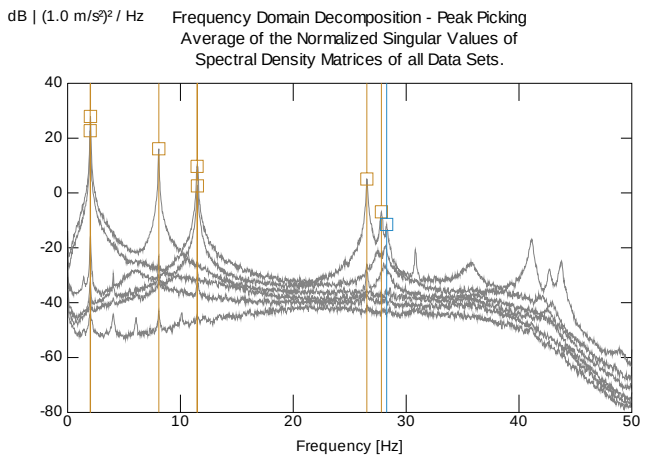

Figure 3 *Frequency Domain Decomposition of measurements on lattice structure. Mean of normalized singular values of spectral density matrices, 2048 frequency lines.*

Table 1 *Experimental and FE determined eigenfrequencies, percentage deviation and MAC-values for experiment on lattice structure.*

$\mathbf{\Phi}$ [–]	f_{exp} [Hz]	f_{FE} [Hz]	Deviation [%]	MAC [–]
1	2.00	2.01	0.5	0.9991
2	2.02	2.02	-0.3	0.7448
3	8.08	7.87	-2.5	0.9791
4	11.47	11.40	-0.6	0.9618
5	11.49	11.54	0.4	0.9671
6	26.51	25.75	-2.9	0.8289
7	27.80	29.49	6.1	0.8714
8	28.27	30.35	7.4	0.8520

Stress spectra are plotted and damage is calculated including all 223 hours of measurements. An example of such a stress spectrum is plotted for channel 1 (leg) in Figure 5, and in Table 2 the damage is listed for all eight channels. The damage is calculated with use of a linear SN-curve with the parameters log K = 16.786 and m = 5 and without any cut-off limit, cf. DS410 [7]. The stress cycles are counted by Rain Flow Counting.

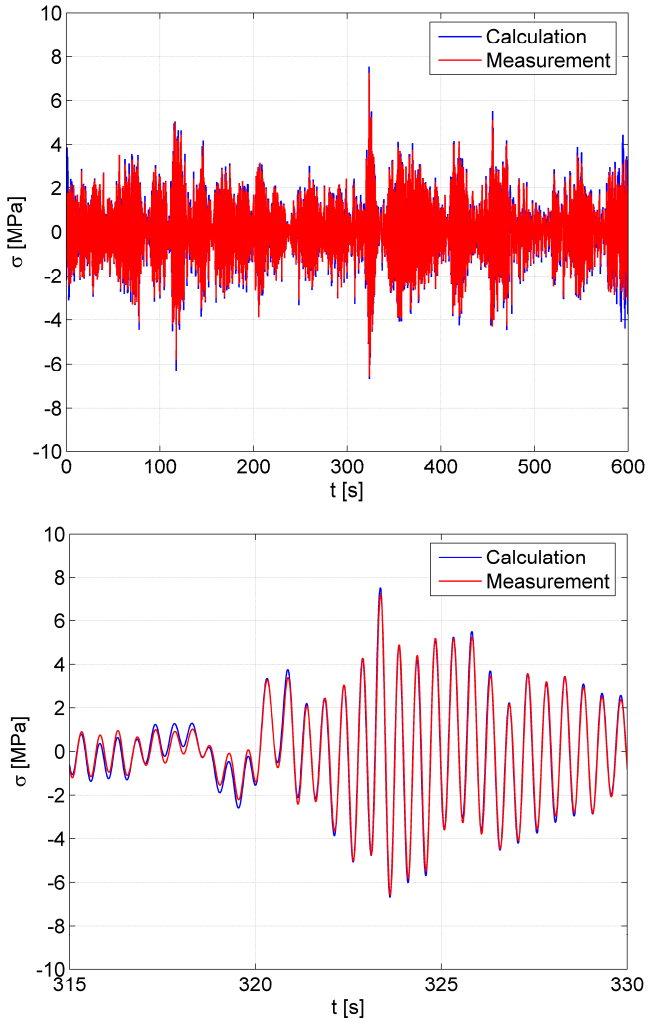

Figure 4 *Example of measured and calculated stress history. (Top) Entire time series, (bottom) zoom in on 315-330 s.*

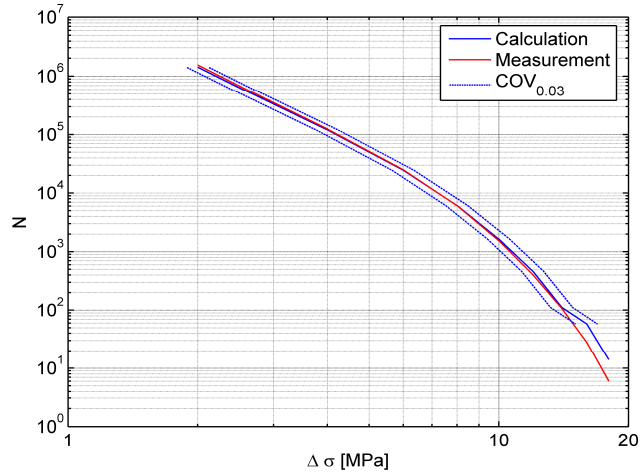

Figure 5 *Example of stress spectrum (channel 1, leg).*

Illustration the large reduction of the uncertainty on the load history and transfer function, COV_{load} = 0.03 is plotted in Figure 5 and listed in Table 2, showing that the calculations for all channels lie below this limit. The COV_{load} is calculated by assuming that the uncertainty is modeled by a normal distributed 95% double-sided probability interval.

Table 2 *Comparison of measured and calculated damage. The ± values indicates the 95% probability intervals for COV_{load} = 0.03.*

Ch. [–]	D_{meas} $1 \cdot 10^{-6}$	D_{calc} $1 \cdot 10^{-4}$
1	3.53	3.54+1.17/-0.93
2	3.55	3.43+1.14/-0.89
3	4.52	3.43+1.14/-0.89
4	0.88	0.73+0.24/-0.19
5	0.86	0.72+0.24/-0.19
6	3.38	3.54+1.17/-0.92
7	2.31	2.74+0.90/-0.72
8	2.22	2.22+0.74/-0.58

6. Example of Reduction in Inspection Costs by Modal Based Fatigue Monitoring

It has been verified with the experiment on the lattice pylon structure that COV_{load} can be reduced to less than 0.05 by modal based fatigue monitoring. In this section it is shown how the number of required inspection decrees by reducing COV_{load} by modal based fatigue monitoring. As example 12 different K-joints are considered, representing 12 joints of a typically offshore steel structure, cf. Table 3.

The reduction in number of inspections is calculated, assuming that COV_{load} is reduced from 0.15 to 0.05 and that the prior calculated equivalent stress range $\Delta\sigma^e$ equals the "measured" equivalent stress range by modal based fatigue monitoring.

The inspection-planning is made with use of the pre-defined generic inspection-plans collected in iPlan. The inspection-plans are based on the parameters in Table 3 and following assumptions:

- Joints are located under water.
- Initial crack length a_0 = 0.1 mm.
- Inspection type and associated POD-curve: MPI.
- Service life T_L = 40 years.
- Fatigue Design Factor *FDF*: 3 or 5.

Table 3 *Parameters for inspection plans.*

ID	COV_{SCF} [-]	Thickn. [m]	*DoB* [-]	T_F [year]	Thresh. [pf/yr]	RIF [-]
a	0.10	0.050	0.50	180	1.0E-05	0.60
b	0.10	0.050	0.50	300	1.0E-05	0.60
c	0.15	0.050	0.50	180	1.0E-05	0.60
d	0.15	0.050	0.50	300	1.0E-05	0.60
e	0.10	0.010	0.50	180	1.0E-05	0.60
f	0.10	0.010	0.50	300	1.0E-05	0.60
g	0.15	0.010	0.50	180	1.0E-05	0.60
h	0.15	0.010	0.50	300	1.0E-05	0.60
i	0.10	0.015	0.50	180	1.0E-05	0.60
j	0.10	0.015	0.50	300	1.0E-05	0.60
k	0.15	0.015	0.50	180	1.0E-05	0.60
l	0.15	0.015	0.50	300	1.0E-05	0.60

Table 4 *Comparison of the two inspection plans.*

COV_{load} [–]	No. of insp. [–]	No. of insp. years [–]
0.05	3	1
0.15	17	10

In Figure 7 the two inspection plans with COV_{load} = 0.05 and COV_{load} = 0.15 are listed and in Table 4 the number of inspections and inspection years are counted. As seen the total number of inspections is reduced from 17 to 3 by reducing COV_{load}, giving a reduction of 82%. Furthermore it is important to notice that the years, when inspections are required, are reduced with 95% from 10 to 1, giving large savings on the initial (startup) inspections costs.

7. Conclusions

It is shown how the number of inspections in risk based inspection planning directly depends on the uncertainty on the load history. It is verified by experiments on a wind loaded lattice pylon structure that the uncertainty can be significantly reduced by determining the stress history by modal based fatigue monitoring. By making inspection plans for typically joints in an offshore steel structure it is estimated that the number of required inspections is reduced with more than 50% by combining modal based fatigue monitoring with risk based inspection planning.

References

[1] Graugaard-Jensen, J., Hjelm, H. P. and Munch, K. (2004). *Modal Based Fatigue Estimation.* M.Sc. thesis, Aalborg University, Denmark.

[2] Graugaard-Jensen, J., Hjelm, H. P. and Munch, K. (2004). *Fatigue Estimation by Natural Input Analysis.* www.svibs.com.

[3] Faber, M.H., Straub, D., Sørensen, J.D. and Tychsen, J. (2003). *Field Implementation of RBI for Jacket Structures.* Proc. OMAE'03, Cancun, Mexico, paper 37304.

[4] Nordic Committee on Building Regulations, NKB (1978). *Recommendations for loading and safety regulations for structural design.* NKB-Report, No. 36, Copenhagen.

[4] Newmann, J. and Raju, I. (1981). *An Empirical Stress-Intensity Factor for the Surface Crack.* Engineering Fracture Mechanics, Vol. 22, No. 6, pp. 185-192.

[5] Smith, I.J. and Hurtworth, S.J. (1981). *Probabilistic Fracture Mechanic Evaluation of Fatigue from Weld Defects in Butt Welded Joints.* Proc. Fitness for Purpose Validation of Welded Constructions, London.

[6] Aaghaakouchak, A., Glinka, G. and Dharmavasan, S. (1989). *A load shedding model for fracture mechanics analysis of fatigue cracks in tubular joints.* Proc. OMAE'89, The Hague, pp. 159-165.

[7] Lassen, T. (1997). *Experimental Investigation and Stochastic Modeling of the Fatigue Behavior of Welded Steel Joints.* PhD thesis, Structural Reliability Theory, paper No. 182, Aalborg University.

[8] Van Overschee, P. and De Moor, B. *Subspace Identification for Linear Systems: Theory, Implementation Applications*. Kluwer Academic Publishers, 1996.

[9] Brincker, R., Zhang, L. and Andersen, P. (2001). *Modal identification of output-only systems using frequency domain decomposition.* Smart Materials and Structures 10 (2001) pp. 441–445.

[10] Kreyszig, E. (1998). *Advanced Engineering Mathematics.* John Wiley & Sons, 8th edition.

[11] DS410, *Standard for Load on Structures DS410*, Danish Standard, 4th edition, 1998.

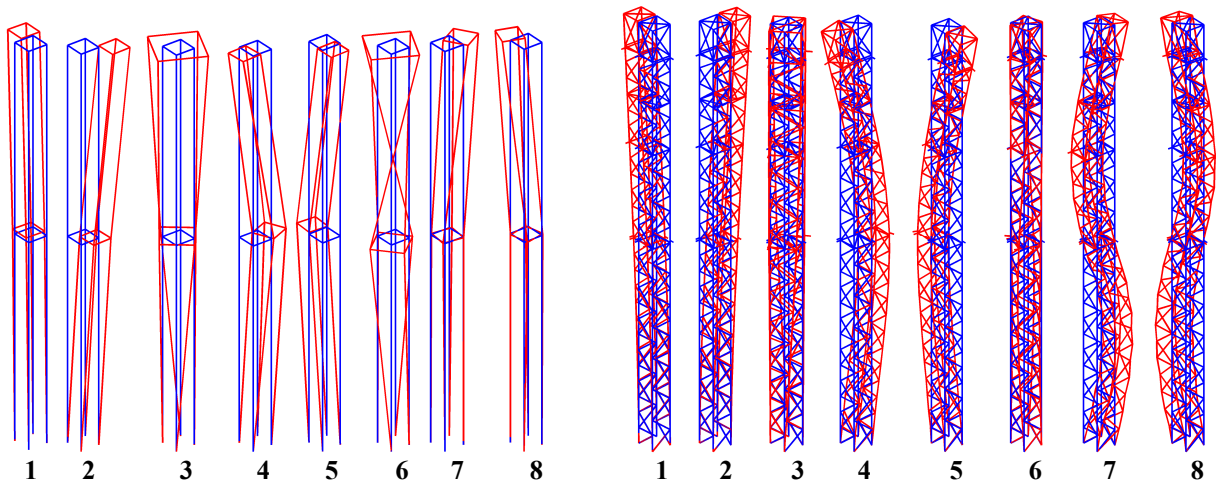

Figure 6 *The eight experimental (left) and numerical (right) mode shapes of the lattice pylon structure.*

ID	Year	2000	2001	2002	2003	2004	2005	2006	2007	2008	2009	2010	2011	2012	2013	2014	2015	2016	2017	2018	2019	2020	2021	2022	2023	2024	2025	2026	2027	2028	2029	2030	2031	2032	2033	2034	2035	2036	2037	2038	2039	2040
a																																										
b																																										
c																																		x								
d																																										
e																																										
f																																										
g																																		x								
h																																										
i																																										
j																																										
k																																		x								
l																																										

ID	Year	2000	2001	2002	2003	2004	2005	2006	2007	2008	2009	2010	2011	2012	2013	2014	2015	2016	2017	2018	2019	2020	2021	2022	2023	2024	2025	2026	2027	2028	2029	2030	2031	2032	2033	2034	2035	2036	2037	2038	2039	2040
a																											x																x
b																																											
c																			x										x														
d																																x											
e																											x											x					
f																																											
g																			x							x									x								
h																														x												
i																											x											x					
j																																											
k																			x							x										x								
l																														x													

Figure 7 *Inspection plans. (Top) COV_{load} = 0.05, (bottom) COV_{load} = 0.15.*